ResearchGate

See discussions, stats, and author profiles for this publication at: https://www.researchgate.net/publication/26870897

Contribution of the Cytoskeleton to the Compressive Properties and Recovery Behavior of Single Cells

ARTICLE *in* BIOPHYSICAL JOURNAL · OCTOBER 2009

Impact Factor: 3.97 · DOI: 10.1016/j.bpj.2009.07.050 · Source: PubMed

CITATIONS
47

READS
28

3 AUTHORS, INCLUDING:

Gidon Ofek
Rice University
9 PUBLICATIONS **263** CITATIONS

SEE PROFILE

Kyriacos Athanasiou
University of California, Davis
336 PUBLICATIONS **11,767** CITATIONS

SEE PROFILE

Available from: Kyriacos Athanasiou
Retrieved on: 10 January 2016

Contribution of the Cytoskeleton to the Compressive Properties and Recovery Behavior of Single Cells

Gidon Ofek,[†] Dena C. Wiltz,[†] and Kyriacos A. Athanasiou[‡*]
[†]Department of Bioengineering, Rice University, Houston, Texas; and [‡]Department of Biomedical Engineering, University of California, Davis, California

ABSTRACT The cytoskeleton is known to play an important role in the biomechanical nature and structure of cells, but its particular function in compressive characteristics has not yet been fully examined. This study focused on the contribution of the main three cytoskeletal elements to the bulk compressive stiffness (as measured by the compressive modulus), volumetric or apparent compressibility changes (as further indicated by apparent Poisson's ratio), and recovery behavior of individual chondrocytes. Before mechanical testing, cytochalasin D, acrylamide, or colchicine was used to disrupt actin microfilaments, intermediate filaments, or microtubules, respectively. Cells were subjected to a range of compressive strains and allowed to recover to equilibrium. Analysis of the video recording for each mechanical event yielded relevant compressive properties and recovery characteristics related to the specific cytoskeletal disrupting agent and as a function of applied axial strain. Inhibition of actin microfilaments had the greatest effect on bulk compressive stiffness (~50% decrease compared to control). Meanwhile, intermediate filaments and microtubules were each found to play an integral role in either the diminution (compressibility) or retention (incompressibility) of original cell volume during compression. In addition, microtubule disruption had the largest effect on the "critical strain threshold" in cellular mechanical behavior (33% decrease compared to control), as well as the characteristic time for recovery (~100% increase compared to control). Elucidating the role of the cytoskeleton in the compressive biomechanical behavior of single cells is an important step toward understanding the basis of mechanotransduction and the etiology of cellular disease processes.

INTRODUCTION

Biomechanical factors play an important role in healthy cellular function, tissue regeneration efforts, and the etiopathogenesis of a myriad of disease types. Individual cells sense and respond to mechanical changes in their microenvironment through mechanotransduction, whereby mechanical signals are translated to a biologic change (1). The cytoskeleton, composed primarily of actin microfilaments, intermediate filaments, and microtubules, is considered to be an important mediator of mechanical forces in individual cells (2), as well as a supporter of cellular structure and function (3). The cytoskeletal elements have been studied individually in various biological systems to yield their respective mechanical parameters (4–9). Recently, the roles of these cytoskeletal components in relation to their different spatial locations within the cell have also been considered (10). However, the specific contribution of each element to the overall biomechanics of the single cell remains poorly understood.

Many cell types, such as articular chondrocytes, experience high compressive loads during everyday activity (11,12). As the structural basis for cells, the various cytoskeletal elements may each serve an important function in the ability of a cell to resist and recover from mechanical forces. Compression of single cells may result in changes in the organization and characteristics of individual cytoskeletal components (13). The cytoskeleton has also been shown to aid in the transmission of forces to the nucleus during compression (14), resulting in direct strain on the nucleus (15) and, thus, altering the biosynthetic regulation of single cells (16). Though prior research has investigated the role of the cytoskeleton in resisting compression, those studies only examined forces applied locally onto the cell (17,18). However, cells typically experience mechanical forces applied along their entirety (19). Therefore, this study was motivated to examine unique relationships of each cytoskeletal element to the bulk compressive biomechanics of single cells with the goal of clarifying the cytoskeleton's role in mediating forces and reinforcing cellular structure during compression.

It is of further importance to examine the ranges of mechanical perturbation that precipitate anabolic or catabolic cellular pathways. Previous research from our group reported a ''critical strain threshold'' in the mechanical behavior of single chondrocytes (20) at ~30% applied axial strain, wherein the cells are no longer able to fully recover from the applied compressive load. At strains above this level, gene expression patterns also display catabolic characteristics (15,21). Thus, one of the aims of this study is to understand the contribution of the cytoskeleton in modulating this strain threshold, which can be considered akin to a yield point in the stress-strain behavior of the single cell. Moreover, since alterations in cellular mechanical properties may be indicative of degenerative and metastatic changes (22–24), a detailed insight into how individual cytoskeletal components affect the compressive characteristics of single cells may aid in elucidating the underlying mechanisms for

Submitted April 8, 2009, and accepted for publication July 15, 2009.

*Correspondence: athanasiou@ucdavis.edu

Editor: Denis Wirtz.

© 2009 by the Biophysical Society

0006-3495/09/10/1873/10 $2.00

doi: 10.1016/j.bpj.2009.07.050

cellular disease alterations and identifying potential treatments for restoring homeostatic conditions.

The overall objective of this study was to examine the contribution of actin, intermediate filaments, and microtubules to the compressive biomechanical characteristics of single cells. Using an anchorage-dependent cell model, individual chondrocytes were incubated with a cytoskeletal disrupting agent that targeted one of the aforementioned cytoskeletal components, after which the cells were tested for their biomechanical characteristics over a range of applied axial strains. This was accomplished by employing an unconfined compression approach (20,25) to test the hypothesis that each cytoskeletal component would contribute differentially to the compressive properties and behavior of single chondrocytes, based on known dissimilarities in their structure and spatial orientation within chondrocytes (26). Specific emphasis was placed on the role of these cytoskeletal elements in the compressive modulus, apparent Poisson's ratio, apparent compressibility, volumetric changes, and recovery behavior of the cells.

MATERIALS AND METHODS

Cell isolation and seeding

Articular cartilage was harvested from 15 adult bovine fetlock joints obtained from a local abattoir (Doreck and Sons Packing, Santa Fe, TX). Single chondrocytes were isolated from the middle/deep region of the cartilage tissue as previously described (20). After tissue digestion, chondrocytes were counted and resuspended at a concentration of 200,000 cells/ml in supplemented DMEM (0.1 mM NEAA, 100 U/ml penicillin/streptomycin, and 0.25 μg/ml fungizone), which either contained a cytoskeletal disrupting agent—cytochalasin D (2 μM) for actin microfilaments, acrylamide (40 mM) for intermediate filaments, or colchicine (10 μM) for microtubules—or did not (control). The concentrations for the specific disrupting agents were chosen based upon prior literature demonstrating their efficacy with isolated chondrocytes (27–29). Chondrocytes were then seeded for 3 h on cut-glass slides, which were placed inside a six-well plate at 37°C and 10% CO_2. The 3 h incubation period has been demonstrated by our group to be sufficient to achieve proper cell attachment for cytocompression testing (30).

Immunocytochemistry

Fluorescent staining was performed to observe the effectiveness of cytochalasin, acrylamide, and colchicine at disrupting actin microfilaments, intermediate filaments, and microtubules, respectively. Chondrocytes were seeded with each cytoskeletal disrupting agent or control in a manner similar to that used for compressive testing. After 3 h of culture, cells were fixed with 4% paraformaldehyde, blocked with 10% FBS, and permeabilized with 0.1% Triton X-100. Cells were then incubated with AlexaFluor 647 phalloidin (Invitrogen, Carlsbad, CA) for actin visualization, paclitaxel (Molecular Probes, Eugene, OR) for microtubule detection, mouse antivimentin primary antibody (Invitrogen) followed by a goat antimouse secondary antibody (Alexaflour 488, Invitrogen) for intermediate filament imaging, and Hoescht's dye for nuclei staining. These slides were viewed with an Axioplan 2 microscope (Carl Zeiss, Oberkochen, Germany). All images for the same fluorescent stain were acquired at the same exposure time and analyzed using Metamorph 4.15 (Universal Imaging, Downingtown, PA).

Unconfined cytocompression and videocapture

A previously described cytocompression device (20) was utilized to apply a range of compressive strains (~5–60%) onto single chondrocytes via a tungsten probe 50.8 μm in diameter. The probe consists of a cantilever beam (of length 2.5 cm) that is bent at its distal end by 90°, resulting in a compressing tip (of length 2 mm). Glass slides were transferred from the six-well plate and positioned upright in a petri dish containing supplemented DMEM with 30 mM HEPES buffer solution and either cytochalasin D (2 μM), acrylamide (40 mM), colchicine (10 μM), or no agent (control cells). The petri dish was then placed on the stage of an IMT-2 inverted microscope (Olympus America, Melville, NY). Individual cells on the glass slide were brought into focus with a 40× objective and then positioned in close proximity to the probe's compressing tip (~5–10 μm away) (Fig. 1). A piezoelectric motor drove the probe a prescribed distance (12–16 μm) axially toward the cell at a rate of 4 μm/s. Based on the initial distance between the probe and the cell, and the prescribed displacement of the probe, each cell could be exposed to a different level of compressive strain. The probe compressed the cell for 30 s and then returned to its original position. After compression, chondrocytes were allowed to recover for 60 s. The entire compression and recovery event was recorded through an AVC-D7 CCD camera (Sony USA, New York, NY) connected to the microscope. The CCD camera provided an additional 10× digital enlargement, yielding a final magnification of 400×. Videos were saved as an AVI file at 640 × 480 resolution for subsequent analysis.

Video analysis and biomechanical measurements

Individual frames from the videos were extracted using Videomach 4.0.2 software (Gromada.com). Images of the initial cell-probe configuration, initial cell-probe contact, cell-probe contact at equilibrium compression, cell immediately after probe release, and cellular recovery every 4 s thereafter were examined. The dimensions of the cell and/or probe positions in each frame were marked using Microsoft Paint 5.1 (Microsoft, Redmond, WA). A pixel/micron ratio of 7.0 was employed in all subsequent analysis of images, and the accuracy of the measurements was deemed to be 2 pixels.

Cantilever beam theory was employed to determine the reaction force of the cell to the probe at peak compression:

$$F = \frac{3EI}{L^3}\delta, \tag{1}$$

where E (Young's modulus), I (area moment of inertia or second moment of inertia), and L (cantilever beam length) are known parameters of the tungsten probe. The Young's modulus, area moment of inertia, and length of the probe used in these experiments were 394.5 GPa, 3.27×10^{-19} m^4, and 2.5 cm, respectively. The deflection of the cantilever (δ) was determined by comparing the true displacement of the probe (via video analysis) with the prescribed piezoelectric displacement (between 12 and 16 μm). Applied stress (σ_a) was estimated as the cell's reaction force divided by its initial cross-sectional area, as in our previous studies (25,31).

Cells were approximated as ellipsoids, with rotational symmetry about their z axis (perpendicular to the plane of seeding), similar to previous methodologies (20,25). Moreover, this basic shape was assumed to be maintained throughout the course of compression and cellular recovery. Thus, using the equation for an ellipsoid with two identical axes, cell volume was calculated as

$$V = \frac{1}{6}\pi h d^2, \tag{2}$$

where h represents the cell's height (or ellipsoid length in the z direction) and d is the cell diameter (or ellipsoid length in the x and y directions). Cell volume was measured at initial setup (V_o), during compression (V_1), and at equilibrium recovery (V_r). Using these volume measurements, a normalized volume change, $(V_o - V_1)/V_o$, and recovered volume fraction, V_r/V_o, were calculated.

The axial strain (ε_a) applied to each cell was determined by the difference in probe position between the initial cell contact and at equilibrium compression, divided by the initial cell height. Lateral strain (ε_l) was defined as the difference between initial cell width and cell width during equilibrium

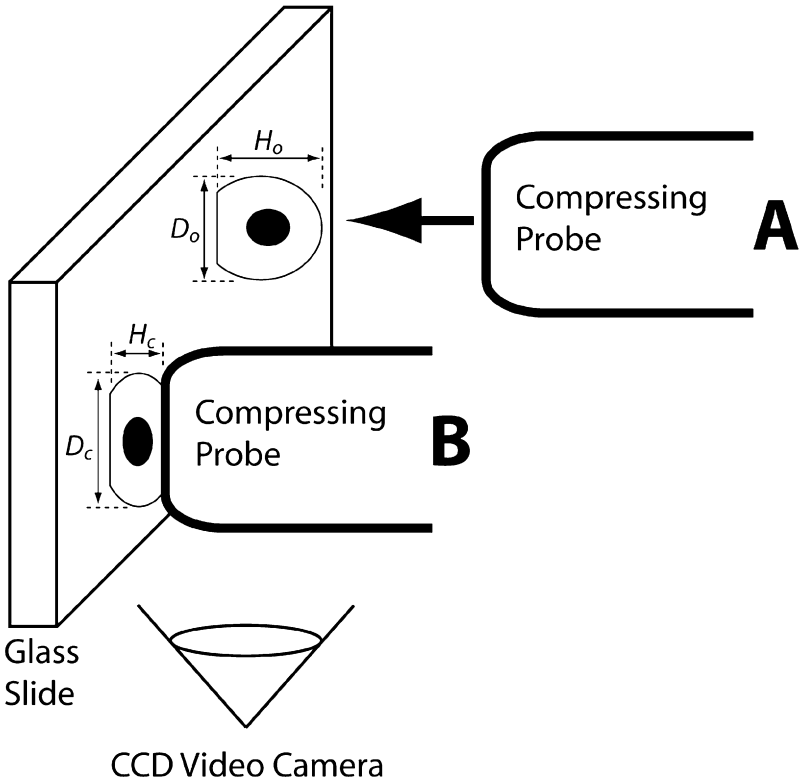

FIGURE 1 Illustration of the cytocompression setup. (*A*) A piezoelectric actuator was used to drive a compressing probe axially toward articular chondrocytes seeded onto glass slides. (*B*) Cells were exposed to compressive strains, generally ranging between 10% and 60%, for 30 s. The cell's height (*H*) and width (*W*) were recorded before and during compression, and the recorded values were used in the calculations for axial and lateral strain. After the probe was removed, the cells were allowed to recover to equilibrium and their recovering heights and widths were continually recorded. The entire mechanical event was captured via a CCD video camera connected to the microscope. The figure is not drawn to scale.

compression, divided by initial cell width. Using these values, the apparent Poisson's ratio (ν_a) was calculated as

$$\nu_a = -\frac{\varepsilon_l}{\varepsilon_a}. \quad (3)$$

To identify the specific relationship between the apparent Poisson's ratio and compressibility changes, an apparent compressibility value (β_a) for each cell was defined as

$$\beta_a = \frac{(V_o - V_l)/V_o}{\sigma_a}. \quad (4)$$

The capacity of the cell to regain its height after different magnitudes of compressive strain was further examined. Upon release of the probe, the recovery strain history, $\varepsilon(t)$, defined as the change in cell height divided by the cell's initial height, was monitored every 4 s and fit to a generalized time-decaying exponential function using MATLAB R2007b (The MathWorks, Natick, MA):

$$\varepsilon(t) = Ae^{-t/\tau} + \varepsilon_r, \quad (5)$$

where A is the recovery coefficient, t is the time in seconds, τ is the characteristic recovery time constant for the cell, and ε_r is the equilibrium residual strain.

Data analysis

Power analysis performed before this study suggested a sample size of $n = 30$ for experimental groups. Briefly, power analysis is a statistical tool used to predict the minimum number of samples needed to observe significant differences between experimental groups, based on expected deviations in cellular mechanical properties (25), a desired significance level ($\alpha = 0.05$), and statistical power ($1 - \beta = 0.80$). All subsequent statistical analyses were performed using Microsoft Office Excel 2003. Linear regression was used to determine whether the equilibrium stress, apparent Poisson's ratio, recovered volume fraction, and residual strain varied as functions of applied axial strain and to test the effects of the cytoskeletal disrupting agents on these functions. Change-point analysis was further used to determine whether a critical threshold of applied axial strain existed at which the biomechanical behavior of single cells was irreversibly changed. As previously described (20), this approach involved performing a series of linear regressions on overlapping segments of data (versus applied strain) to look for potential changes in slope. If a discontinuity was apparent, the original data were separated into two subsets, each of which was analyzed with linear regression to identify whether these resultant lines exhibited different correlations with applied strain. An effect of axial strain was considered significant if $p \leq 0.05$. In addition, linear regression was similarly used to assess the relationship between apparent compressibility and apparent Poisson's ratio.

RESULTS

In this study, a total of 128 cells were tested singly over a range of applied strains (30 cells for control, 34 for cytochalasin treatment, 30 for acrylamide treatment, and 34 for colchicine treatment). Cells were examined for their compressive properties and recovery behavior through video analysis of the mechanical event (Fig. 2). Representative recovery curves for control cells that incurred either low or high applied strains are shown in Fig. S1 in the Supporting Material. Note the substantially different recovery behavior below and above the critical strain threshold. Salient compressive properties and recovery characteristics for each treatment group are summarized in Table 1.

Cytoskeletal disruption

Through immunocytochemistry, we confirmed that the chosen cytoskeletal disrupting agents, at their respective

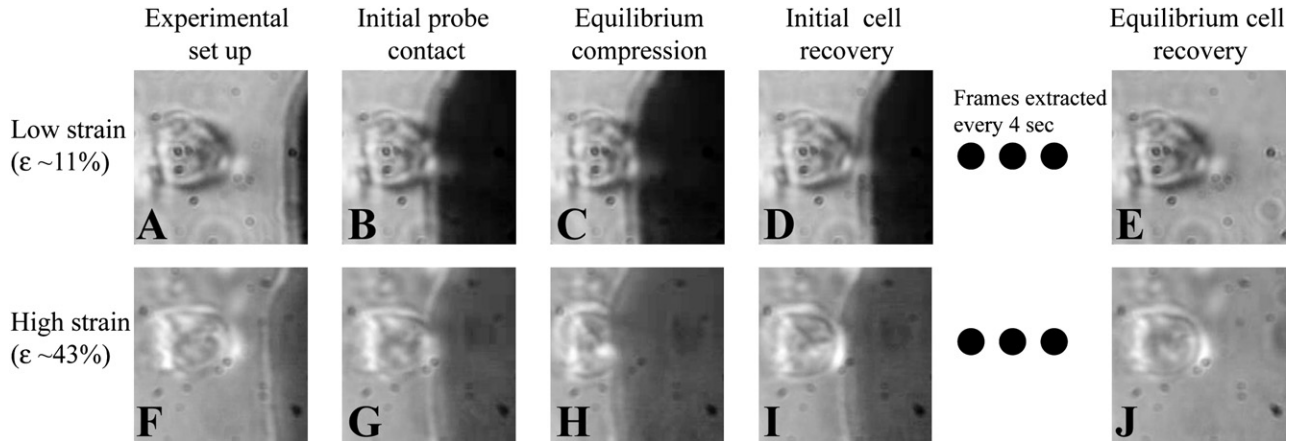

FIGURE 2 Single-cell compression and recovery behavior. The entire mechanical event was video-recorded and subsequently analyzed to yield mechanical properties and indicators for recovery behavior. Differences can be observed between cells experiencing low strain (*A–E*) and high strain (*F–J*). The initial experimental set up (*A* and *F*), initial probe contact (*B* and *G*), and equilibrium compression (*C* and *H*) provide information on the compressive properties of the cells based on monitored changes in the cell shape and the movement of the probe. Upon release of the probe (*D* and *I*), the cell's recovery behavior was tracked every 4 s until equilibrium was reached (*E* and *J*).

concentrations, were effective in predominately disturbing their targeted cytoskeletal element (Fig. S2). Although it should be noted that treatment with each cytoskeletal disrupting agent affected all cytoskeletal elements, not just the targeted one, the secondary effects of the disrupting agents were minimal compared to their effect on the targeted cytoskeletal element. Consistent with prior reports (28,32,33), cytochalasin treatment broke down actin microfilaments into spotty aggregates, acrylamide collapsed the intermediate filament network, and colchicine substantially decreased the overall intensity of microtubule staining.

Cell size and morphology

Generally, the acrylamide or colchicine treatment did not affect chondrocyte size or rounded morphology, with

TABLE 1 Salient compressive properties and recovery behavior characteristics for cells experiencing actin, intermediate filament, or microtubule disruption

	Biomechanical characteristic	Mechanical indicator	Control	AF disruption (cytochalasin)	IF disruption (acrylamide)	MT disruption (colchicine)
	Stiffness	Compressive modulus (kPa)	1.63 ± 0.31	1.01 ± 0.10*	1.69 ± 0.14	1.39 ± 0.19
	Initial compressibility	Apparent Poisson's ratio at $\varepsilon_a = 0$	0.49 ± 0.08	0.49 ± 0.07	0.50 ± 0.05	0.36 ± 0.06*
	Strain-dependent compressibility	Apparent Poisson's ratio slope	−0.47 ± 0.25	−0.47 ± 0.22	−0.03 ± 0.22*	−0.33 ± 0.16
	Yield in recovery behavior	Critical strain threshold, $\varepsilon_{crit,}$ (%)	20	25	30	20
Generalized recovery behavior characteristics below critical threshold, $\varepsilon(t) = Ae^{-t/\tau} + \varepsilon_r$	Initial strain (for $\varepsilon_a < \varepsilon_{crit}$)	Recovery coefficient (A)	0.17 ± 0.09	0.15 ± 0.05	0.17 ± 0.05	0.11 ± 0.03
	Recovery duration (for $\varepsilon_a < \varepsilon_{crit}$)	Characteristic recovery time, τ (s)	1.6 ± 1.3	1.9 ± 0.8	2.9 ± 1.6*	4.1 ± 1.8*
	Permanent deformation (for $\varepsilon_a < \varepsilon_{crit}$)	Residual strain, ε_r (%)	1.1 ± 1.6	2.3 ± 2.5	2.4 ± 1.8	2.2 ± 1.3
Generalized recovery behavior characteristics above critical threshold, $\varepsilon(t) = Ae^{-t/\tau} + \varepsilon_r$	Initial strain (for $\varepsilon_a > \varepsilon_{crit}$)	Recoverycoefficient (A)	0.33 ± 0.07	0.29 ± 0.07	0.34 ± 0.08	0.25 ± 0.09
	Recovery duration (for $\varepsilon_a > \varepsilon_{crit}$)	Characteristic recovery time, τ (s)	1.5 ± 1.1	2.4 ± 2.0*	1.8 ± 1.3	2.9 ± 1.8*
	Permanent deformation (for $\varepsilon_a > \varepsilon_{crit}$)	Residual strain, ε_r (%)	7.4 ± 5.2	8.8 ± 7.2	5.9 ± 3.8	9.9 ± 4.2

Compressive moduli and Poisson's ratios are presented as value ± 95% confidence boundary. All other values are presented as mean ± SD. AF, actin microfilaments; IF, intermediate filaments; MT, microtubules; *, significance from control ($p < 0.05$).

cellular heights and widths typically varying between 8 and 12 μm. However, the initial width (W) and volume (V), although not the height (H), of cytochalasin cells ($H = 10.8 \pm 1.6\ \mu$m, $W = 10.7 \pm 1.0\ \mu$m, and $V = 657 \pm 195\ \mu m^3$) were greater ($p < 0.05$) than in control cells ($H = 10.2 \pm 1.3\ \mu$m, $W = 9.7 \pm 0.9\ \mu$m, and $V = 512 \pm 136\ \mu m^3$), acrylamide cells ($H = 10.5 \pm 1.0\ \mu$m, $W = 9.8 \pm 0.9\ \mu$m, and $V = 547 \pm 155\ \mu m^3$), and colchicine cells ($H = 10.2 \pm 2.0\ \mu$m, $W = 9.8 \pm 1.0\ \mu$m, and $V = 522 \pm 164\ \mu m^3$).

Cell stiffness

A compressive modulus for each experimental group was estimated as the slope of equilibrium stress values plotted against the applied axial strain (Fig. 3). Control and cytochalasin-, acrylamide-, and colchicine-treated cells all exhibited a linear correlation between stress and strain ($p < 0.001$), with slopes of 1.63 kPa, 1.01 kPa, 1.69 kPa, and 1.39 kPa, respectively. A difference was observed between the compressive moduli of the control and cytochalasin cells ($p < 0.05$), as indicated by the 95% confidence intervals for those slopes.

Cellular compressibility

Control, cytochalasin, and colchicine cells all displayed compressive material characteristics, whereby volumetric changes were observed in response to the applied compressive load. Moreover, apparent Poisson's ratio (as an indicator of compressibility) decreased as a function of applied strain in the control, cytochalasin, and colchicine groups (Fig. 4). No differences in apparent Poisson's ratio were noted between control and cytochalasin cells. Colchicine treatment resulted in an overall increase in cell volume loss compared to control cells. The intercept of the apparent Poisson's ratio for colchicines-treated cells was lower than that of control cells ($p = 0.05$), as indicated by their 95% confidence intervals. In direct contrast to colchicine treatment, treatment with acrylamide generally caused cells to be incompressible over the entire range of applied axial strains, as no significant linear correlation ($p = 0.73$) was observed and all apparent Poisson's ratio values were ~0.5. Finally, the slope of the apparent Poisson's ratio values for acrylamide cells was different from that of control cells ($p < 0.05$), as indicated by the 95% confidence intervals for these slopes.

The apparent compressibility values for control and cytochalasin- and colchicine-treated cells were around zero at low strains and then increased ($p < 0.001$) with greater applied axial strain (Fig. 5, A, C, and G). Conversely, all apparent compressibility values for acrylamide-treated cells were near zero (Fig. 5 E) and did not exhibit a significant linear correlation with applied axial strain ($p = 0.51$), supporting the previous observation of incompressibility (or no volume loss) over the entire range of applied strains as a result of intermediate filament inhibition. In addition, an inverse relationship was observed between apparent compressibility values and apparent Poisson's ratio (Fig. 5 B, D, F, and H). For low apparent Poisson's ratio values, the apparent compressibility was typically high ($\beta_a > 1$) in control and cytochalasin- and colchicine-treated cells. The apparent compressibility values then decreased toward zero as the apparent Poisson's ratio values approached 0.5.

Cellular recovery behavior

The recovery behavior of cells from all groups was well approximated by the exponential decay function for strain recovered over time, with R^2 values generally between 0.90 and 0.99 (Fig. S1). Residual strains and recovered volumes were further measured once the cell was allowed to recover to equilibrium. Discontinuities in cellular recovery were observed for control, cytochalasin, acrylamide, and colchicine cells at 30%, 25%, 30%, and 20% applied axial strains, respectively. This discontinuity constituted a yield strain, whereby the biomechanical behavior of single chondrocytes was irreversibly changed. Below the yield strain,

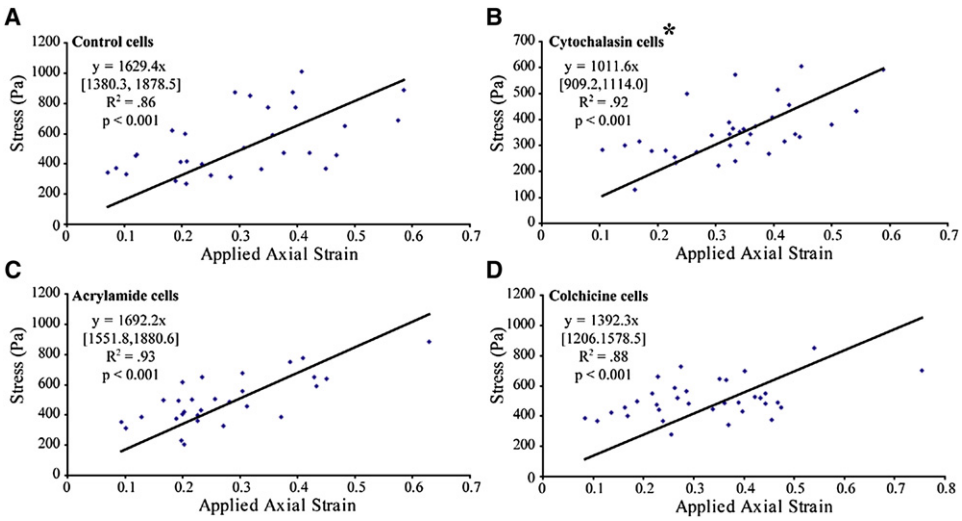

FIGURE 3 Cellular stiffness in response to cytoskeletal disrupting agents. Compressive moduli for each cell type were measured based on the slope between equilibrium stress and applied axial strain. The lower and upper limits for the 95% confidence interval for this slope are listed in brackets. Control (A), and cytochalasin-treated (B), acrylamide-treated (C), and colchicine-treated (D) cells all exhibited a significant linear correlation between stress and strain. Treatment with cytochalasin decreased the compressive modulus of chondrocytes compared to that of control cells (*$p < 0.05$). No differences were observed between the other treatment groups and control cells.

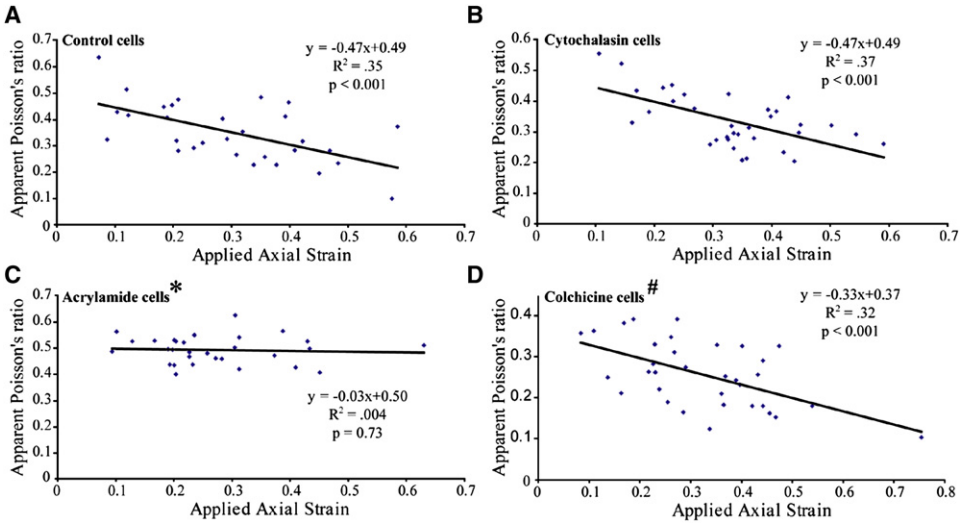

FIGURE 4 Apparent Poisson's ratios in response to cytoskeletal disrupting agents and applied axial strain. Apparent Poisson's ratios decreased as a function of applied strain in control (*A*), and cytochalasin-treated (*B*) and colchicine-treated (*D*) cells. No differences in apparent Poisson's ratio values were observed between control and cytochalasin-treated cells, suggesting that actin does not play a major role in cellular compressibility. Acrylamide-treated cells (*C*) were consistently incompressible ($\nu_a \sim 0.5$) over the entire range of applied strains and exhibited a slope different from that of control cells ($^*p < 0.05$). The intercept for the apparent Poisson's ratio values of the colchicine-treated cells (*D*) was lower than that of control cells ($^\#p = 0.05$), indicating an overall increase in volume loss during compression with colchicine treatment.

chondrocytes were able to recover their original dimensions, in terms of both volume (Fig. 6) and axial strain (Fig. S3). However, above the yield strain, recovered volume fraction and residual strain values exhibited a significant linear correlation with applied strain, indicating a permanent loss in cellular volume and height.

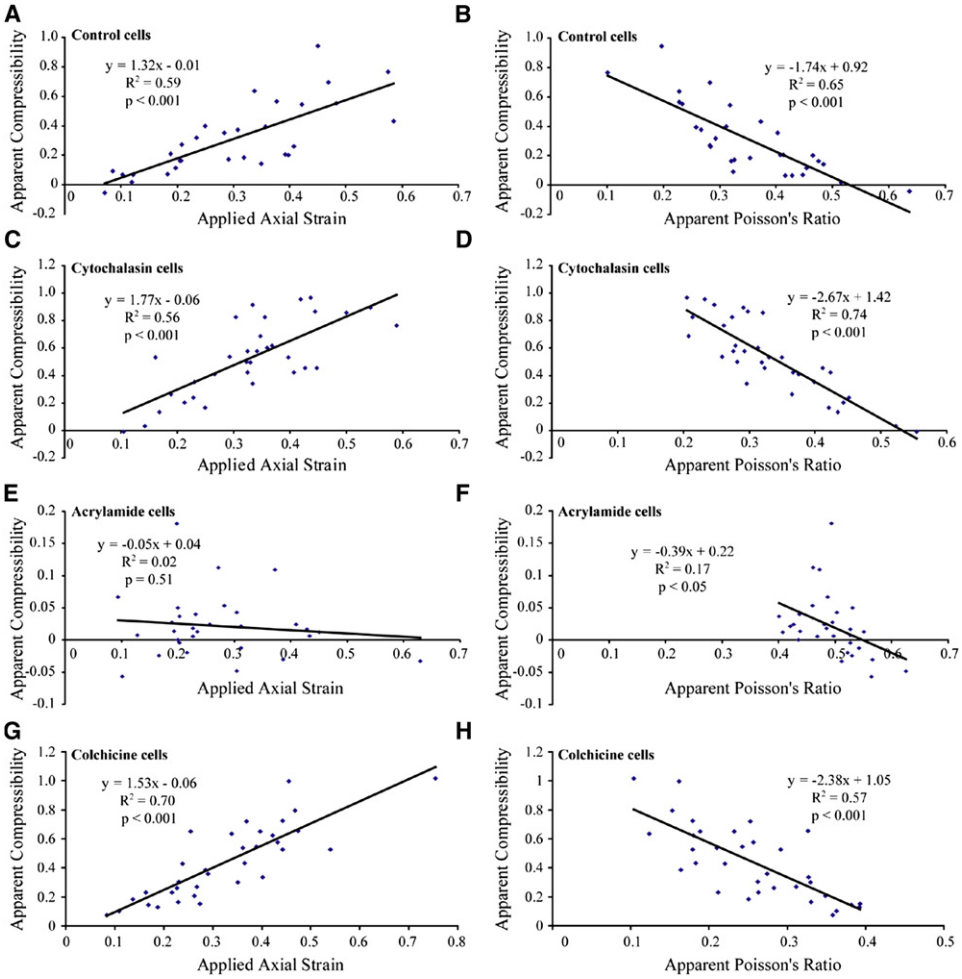

FIGURE 5 Apparent compressibility in response to cytoskeletal disrupting agents and applied axial strain, and relationship of apparent compressibility to apparent Poisson's ratio. At low strains, the apparent compressibility values of control (*A*), cytochalasin-treated (*C*), and colchicine-treated (*G*) cells were all near zero. The apparent compressibility values for each of these treatment groups then increased with greater applied strain, exhibiting a significant linear correlation. In contrast, no correlation was observed between apparent compressibility and applied strain for acrylamide-treated cells (*E*), with all values near zero. Furthermore, the apparent compressibility values of control (*B*), cytochalasin-treated (*D*), acrylamide-treated (*F*), and colchicine-treated (*H*) cells were inversely related to the cell's apparent Poisson's ratio, all exhibiting significant linear correlations.

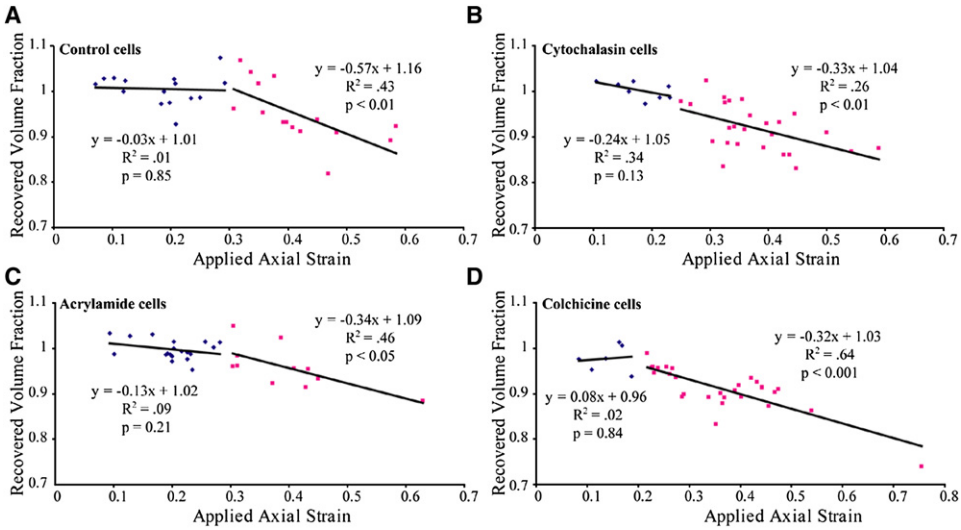

FIGURE 6 Recovered volume fraction behavior in response to cytoskeletal disrupting agents and applied axial strain. Discontinuities in recovered volume fraction were observed for control (*A*), cytochalasin-treated (*B*), acrylamide-treated (*C*), and colchicine-treated (*D*) cells at 30%, 25%, 30%, and 20% applied axial strains, respectively. After the discontinuity, recovered volume fraction values exhibited a significant linear correlation with applied strain, indicating a permanent loss in cell volume.

Cytoskeletal disruption further affected single-cell recovery time constants. Colchicine treatment ($\tau = 3.2 \pm 1.8$ s) resulted in the largest increase in recovery time over control cells ($\tau = 1.6 \pm 1.2$ s) ($p < 0.05$), demonstrative of a slowed cellular recovery. Cytochalasin and acrylamide treatment also resulted in an increase in recovery time constant ($\tau = 2.3 \pm 1.8$ s and $\tau = 2.5 \pm 1.6$ s, respectively; $p = 0.09$ for cytochalasin and $p < 0.05$ for acrylamide).

DISCUSSION

Elucidating the role of the cytoskeleton in the mechanical characteristics of single cells may have important ramifications for understanding cellular mechanotransduction, as well as cell structure and function. This study was designed to examine the contribution of actin, intermediate filaments, and microtubules to the mechanical properties and recovery behavior of individual chondrocytes, over a range of applied compressive strains. Several notable observations were made in this study pertaining to the compressive biomechanical nature of single cells. First, we identified actin microfilaments as the greatest contributor to bulk cell stiffness, as measured by the compressive modulus, during unconfined cytocompression. Second, intermediate filaments and microtubules were each found to play a central function in cellular volumetric changes or compressibility, as measured by the apparent Poisson's ratio. Third, microtubule disruption had the largest effect on the transition from recoverability to permanent cell deformation, as measured by the critical strain threshold in cellular recovery behavior. Finally, it was shown that all of the cytoskeletal elements are needed to maintain the time for recovery from a compressive force, with microtubules exerting the most influence.

Actin microfilaments were observed to play a significant role in the compressive stiffness of single cells. The removal of actin decreased the cell compressive modulus, compared to control, whereas inhibition of microtubules and intermediate filaments had little effect on this parameter. Prior research has shown a correlation between actin inhibition and cell stiffness under tension (29,34) or point indentation (17), but not under a bulk cell testing modality that considers the typical compressive in vivo loading conditions in musculoskeletal tissues. Differences in the role of each cytoskeletal element in overall cell compressive stiffness may be attributable to their respective locations and structure. Actin is positioned primarily along the periphery of the cell, where it provides mechanical reinforcement for the cytoplasm (26,35). Conversely, microtubules are formed from α- and β-tubulin arranged into protofilaments and can be generally thought of as structural rods (36). These rods, however, may be more loosely distributed when compared to the tighter actin network that is found throughout the cell (26). Thus, this looseness of the microtubule meshwork and tightness of the actin network may underlie the difference between the contributions of these two cytoskeletal elements to cell stiffness. In contrast, intermediate filaments form coiled-coil structures, known to have flexible regions at their head and tail (37), and act primarily by resisting tensile forces (34). Identifying the cytoskeletal contributors to cell stiffness is important since this property may influence cell behavior (30,38) and can be an indicator of cell pathology (23). Cellular stiffness can play a critical role in the cell's interpretation of mechanical stimuli, which are known to precipitate regenerative (39) or degenerative pathways (15). Furthermore, by elucidating the contributors to bulk cell stiffness, research can be performed to enhance a cell's ability to function under mechanical environments related to either regenerative or pathologic conditions.

To our knowledge, this is the first study to demonstrate that cellular compressibility is maintained through a balance of intermediate filaments and microtubules. We observed that the removal of intermediate filaments caused cells to become incompressible ($\nu_a = 0.5$, $\beta_a = 0$) over the entire range of applied strains, whereas inhibition of microtubules

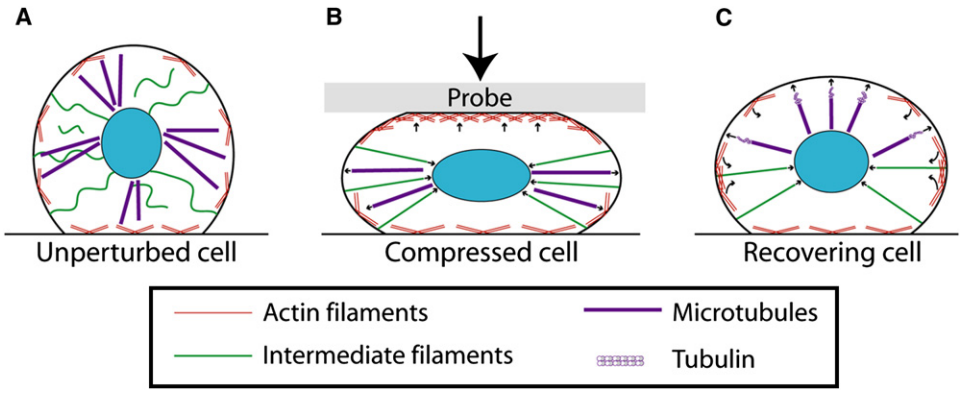

FIGURE 7 Proposed role of actin microfilaments, intermediate filaments, and microtubules in cell compression and recovery. (*A*) When the cell is unperturbed, actin microfilaments are positioned cortically, intermediate filaments connect the nucleus to the cell membrane, and microtubules function as rigid struts. (*B*) Under compression, actin microfilaments reorganize themselves along the interface of the cell and probe to directly resist the compressive force. Meanwhile, intermediate filaments become tense and exert an inward force, limiting the transverse expansion of the cell. Conversely, microtubules push outward during compression, thereby supporting a greater maintenance of the original cell volume. (*C*) During recovery, actin microfilaments and intermediate filaments pull the cell to its original shape through their tensile actions. Moreover, microtubules extend outward and upward through tubulin polymerization to enhance cell recovery, and to facilitate the relocalization of organelles or other cytoskeletal elements. Arrows indicate the direction of the normal force generated by each cytoskeletal element during compression or recovery.

induced an overall downward shift in the apparent Poisson's ratio values. Mechanistically, this means that intermediate filaments serve as tensile elements, akin to ropes, that aid in ''pulling'' the cell together (40), thereby limiting the translation of axial to lateral strain. Conversely, microtubules act as solid rods (41) that facilitate an outward ''push'' during axial compression and thus, a greater retention of the original cell volume. Therefore, considering the pattern of decreasing apparent Poisson's ratio values with increased compressive strain in control cells, our results suggest that this may be due to a breakdown of the microtubule network at high strains (42). Understanding the functional role of the cytoskeleton in cellular compressibility is of particular relevance since cell volume changes may influence cellular homeostasis and tissue matrix production (43). However, it is important to note that other factors besides the cytoskeleton, such as intracellular osmotic levels and active volume regulation mechanisms (44), may affect cellular compressibility and induce an exudation of the cytosol.

Identifying the range of mechanical forces that induce changes in cellular behavior is critical in developing appropriate loading regimens in functional tissue engineering or understanding disease etiology. After the observed critical threshold in all experimental groups, cellular residual strain and recovered volume fraction exhibited a significant dependence on applied strain. In terms of classical engineering mechanisms, this threshold represents a yield point at which the cells incur a permanent or ''plastic'' deformation (45). Conversely, below this threshold, cells retain their original volume and shape after compression; thus, they can be mechanically stimulated for regenerative purposes (46). Based on our results, this critical-strain threshold in cell mechanical behavior may be primarily due to a loss of structural stabilization by microtubules. In this study, the inhibition of microtubules resulted in the largest shift of the critical-strain threshold, from 30% to 20% compressive strain. It has been previously shown that microtubules aid in maintaining cell shape and serve as a ''scaffold'' for other cytoskeletal elements (26). Thus, at this yield strain, microtubules may buckle (47), resulting in the inability of cells to fully recover from the applied force. Indeed, prior research has demonstrated that microtubules will buckle in response to compressive loads applied along the cell's membrane (41). Moreover, using optical bead experiments on individual microtubules, researchers have determined that this cytoskeletal element buckles under directly applied compressive forces ranging between 0.5 and 1.5 pN (48). Identifying microtubules as the largest contributor to cell recovery behavior may have important implications for regenerative medicine. Future researchers may employ biochemical agents to directly target microtubules to help cells recover from unphysiological loads.

All cytoskeletal elements appear to play a role in the recovery time of single chondrocytes in response to a compressive load, with microtubules exerting the largest influence. Removal of microtubules doubled the cellular recovery time constant, and inhibition of actin and intermediate filaments led to a 50% increase in this time constant. Microtubules, which are spread throughout the cell, are used as guides for the localization of other cellular structures (36) and act as a trafficking highway for organelles (49). Thus, in the absence of these microtubule pathways, organelles or other cytoskeletal elements may have trouble relocalizing to their initial position. In addition, microtubules are highly dynamic; the addition of α- or β-tubulin subunits to these struts may push on other cytoskeletal elements to enhance cell recovery (50). Conversely, actin and intermediate filaments can facilitate a quick recovery of cellular shape through tension (51). These elements will be stressed as the cell laterally expands during compression. Upon release of the compressing probe, actin and intermediate filaments may contract, thereby aiding the cell's recovery to its original shape. Understanding the contributors to cellular recovery time may provide insight into the mechanisms at

play during dynamic compressive stimulation of both cells and tissues, which has been shown to be beneficial in numerous regenerative applications (46,52). With this information, appropriate loading frequencies may be developed to mirror alterations of the cytoskeleton during phenotypic changes (53,54) and thus promote neotissue growth.

Although studying the mechanical characteristics of single cells may shed light on intracellular mechanisms and cellular homeostasis, the removal of cells from their native environment poses limitations. Isolating individual cells disrupts connections between the cytoskeleton and the extracellular matrix (19,55 and eliminates the role of the cellular microenvironment to appropriately transmit mechanical forces to the cell (56,57). Notwithstanding this caveat, the cytoskeletal organization of single chondrocytes appears to be retained during isolation in monolayer culture (29). In addition, mechanical testing of individual cells makes it possible to discern differences based on pathologic state (22,23), phenotype (54,58), and spatial origin within a tissue (30). Thus, single-cell unconfined cytocompression may be a testing modality useful for examining the mechanical contributions of various cytoskeletal elements, as long as its results are placed within the appropriate context.

This study provides what we believe are new insights into the role of the cytoskeleton in the compressive mechanical characteristics of single cells and the relationship between cellular structure and mechanical function (Fig. 7). Actin microfilaments were observed to be the largest contributor to bulk cell compressive stiffness and cell volume. Meanwhile, intermediate filaments were found to play an important role in cellular compressibility, fettering transverse cell expansion over the entire range of applied axial strains. On the other hand, we found that microtubules contribute to the incompressive nature of cells and maintain the critical-strain threshold and time constant in cellular recovery behavior. Discerning the role of the cytoskeleton in the mechanical properties and behavior of single cells facilitates a greater understanding of cellular biomechanical changes during tissue pathogenesis and regeneration (23,58), as well as the mechanisms for force transmission within the cell (2).

SUPPORTING MATERIAL

Three figures are available at http://www.biophysj.org/biophysj/supplemental/S0006-3495(09)01301-0.

We gratefully acknowledge funding from the National Institute of Arthritis and Musculoskeletal and Skin Diseases (R01 AR053286), the National Institutes of Health (training fellowship for G.O.; 5 T90 DK70121-03 and 5 R90 DK71504-03), and the National Science Foundation (training fellowship for D.C.W.; HRD-0450363).

REFERENCES

1. Jaalouk, D. E., and J. Lammerding. 2009. Mechanotransduction gone awry. *Nat. Rev. Mol. Cell Biol.* 10:63–73.
2. Wang, N., J. P. Butler, and D. E. Ingber. 1993. Mechanotransduction across the cell surface and through the cytoskeleton. *Science.* 260:1124–1127.
3. McBeath, R., D. M. Pirone, C. M. Nelson, K. Bhadriraju, and C. S. Chen. 2004. Cell shape, cytoskeletal tension, and RhoA regulate stem cell lineage commitment. *Dev. Cell.* 6:483–495.
4. Gardel, M. L., F. Nakamura, J. Hartwig, J. C. Crocker, T. P. Stossel, et al. 2006. Stress-dependent elasticity of composite actin networks as a model for cell behavior. *Phys. Rev. Lett.* 96:088102.
5. Brangwynne, C. P., G. H. Koenderink, F. C. Mackintosh, and D. A. Weitz. 2008. Nonequilibrium microtubule fluctuations in a model cytoskeleton. *Phys. Rev. Lett.* 100:118104.
6. Bathe, M., C. Heussinger, M. M. Claessens, A. R. Bausch, and E. Frey. 2008. Cytoskeletal bundle mechanics. *Biophys. J.* 94:2955–2964.
7. Schaap, I. A., C. Carrasco, P. J. de Pablo, F. C. MacKintosh, and C. F. Schmidt. 2006. Elastic response, buckling, and instability of microtubules under radial indentation. *Biophys. J.* 91:1521–1531.
8. Janmey, P. A., U. Euteneuer, P. Traub, and M. Schliwa. 1991. Viscoelastic properties of vimentin compared with other filamentous biopolymer networks. *J. Cell Biol.* 113:155–160.
9. Tseng, Y., and D. Wirtz. 2001. Mechanics and multiple-particle tracking microheterogeneity of α-actinin-cross-linked actin filament networks. *Biophys. J.* 81:1643–1656.
10. Heidemann, S. R., and D. Wirtz. 2004. Towards a regional approach to cell mechanics. *Trends Cell Biol.* 14:160–166.
11. Wu, J. Z., W. Herzog, and M. Epstein. 1999. Modelling of location- and time-dependent deformation of chondrocytes during cartilage loading. *J. Biomech.* 32:563–572.
12. Guilak, F., A. Ratcliffe, and V. C. Mow. 1995. Chondrocyte deformation and local tissue strain in articular cartilage: a confocal microscopy study. *J. Orthop. Res.* 13:410–421.
13. Lee, D. A., M. M. Knight, J. F. Bolton, B. D. Idowu, M. V. Kayser, et al. 2000. Chondrocyte deformation within compressed agarose constructs at the cellular and sub-cellular levels. *J. Biomech.* 33:81–95.
14. Guilak, F. 1995. Compression-induced changes in the shape and volume of the chondrocyte nucleus. *J. Biomech.* 28:1529–1541.
15. Leipzig, N. D., and K. A. Athanasiou. 2008. Static compression of single chondrocytes catabolically modifies single-cell gene expression. *Biophys. J.* 94:2412–2422.
16. Buschmann, M. D., E. B. Hunziker, Y. J. Kim, and A. J. Grodzinsky. 1996. Altered aggrecan synthesis correlates with cell and nucleus structure in statically compressed cartilage. *J. Cell Sci.* 109:499–508.
17. Wu, H. W., T. Kuhn, and V. T. Moy. 1998. Mechanical properties of L929 cells measured by atomic force microscopy: effects of anticytoskeletal drugs and membrane crosslinking. *Scanning.* 20:389–397.
18. Hemmer, J. D., J. Nagatomi, S. T. Wood, A. A. Vertegel, D. Dean, et al. 2009. Role of cytoskeletal components in stress-relaxation behavior of adherent vascular smooth muscle cells. *J. Biomech. Eng.* 131:041001.
19. Guilak, F., and V. C. Mow. 2000. The mechanical environment of the chondrocyte: a biphasic finite element model of cell-matrix interactions in articular cartilage. *J. Biomech.* 33:1663–1673.
20. Shieh, A. C., E. J. Koay, and K. A. Athanasiou. 2006. Strain-dependent recovery behavior of single chondrocytes. *Biomech. Model. Mechanobiol.* 5:172–179.
21. Kurz, B., M. Jin, P. Patwari, D. M. Cheng, M. W. Lark, et al. 2001. Biosynthetic response and mechanical properties of articular cartilage after injurious compression. *J. Orthop. Res.* 19:1140–1146.
22. Cross, S. E., Y. S. Jin, J. Rao, and J. K. Gimzewski. 2007. Nanomechanical analysis of cells from cancer patients. *Nat. Nanotechnol.* 2:780–783.
23. Trickey, W. R., G. M. Lee, and F. Guilak. 2000. Viscoelastic properties of chondrocytes from normal and osteoarthritic human cartilage. *J. Orthop. Res.* 18:891–898.
24. Darling, E. M., S. Zauscher, J. A. Block, and F. Guilak. 2007. A thin-layer model for viscoelastic, stress-relaxation testing of cells using

atomic force microscopy: do cell properties reflect metastatic potential? *Biophys. J.* 92:1784–1791.

25. Koay, E. J., G. Ofek, and K. A. Athanasiou. 2008. Effects of TGF-β1 and IGF-I on the compressibility, biomechanics, and strain-dependent recovery behavior of single chondrocytes. *J. Biomech.* 41:1044–1052.
26. Langelier, E., R. Suetterlin, C. D. Hoemann, U. Aebi, and M. D. Buschmann. 2000. The chondrocyte cytoskeleton in mature articular cartilage: structure and distribution of actin, tubulin, and vimentin filaments. *J. Histochem. Cytochem.* 48:1307–1320.
27. Guilak, F., R. A. Zell, G. R. Erickson, D. A. Grande, C. T. Rubin, et al. 1999. Mechanically induced calcium waves in articular chondrocytes are inhibited by gadolinium and amiloride. *J. Orthop. Res.* 17:421–429.
28. Madsen, K., S. Moskalewski, J. Thyberg, and U. Friberg. 1979. Comparison of the in vitro effects of colchicine and its derivative colchiceine on chondrocyte morphology and function. *Experientia.* 35:1572–1573.
29. Trickey, W. R., T. P. Vail, and F. Guilak. 2004. The role of the cytoskeleton in the viscoelastic properties of human articular chondrocytes. *J. Orthop. Res.* 22:131–139.
30. Shieh, A. C., and K. A. Athanasiou. 2006. Biomechanics of single zonal chondrocytes. *J. Biomech.* 39:1595–1602.
31. Leipzig, N. D., and K. A. Athanasiou. 2005. Unconfined creep compression of chondrocytes. *J. Biomech.* 38:77–85.
32. Schliwa, M. 1982. Action of cytochalasin D on cytoskeletal networks. *J. Cell Biol.* 92:79–91.
33. Sager, P. R. 1989. Cytoskeletal effects of acrylamide and 2,5-hexanedione: selective aggregation of vimentin filaments. *Toxicol. Appl. Pharmacol.* 97:141–155.
34. Wang, N. 1998. Mechanical interactions among cytoskeletal filaments. *Hypertension.* 32:162–165.
35. Durrant, L. A., C. W. Archer, M. Benjamin, and J. R. Ralphs. 1999. Organisation of the chondrocyte cytoskeleton and its response to changing mechanical conditions in organ culture. *J. Anat.* 194:343–353.
36. Blain, E. J. 2009. Involvement of the cytoskeletal elements in articular cartilage homeostasis and pathology. *Int. J. Exp. Pathol.* 90:1–15.
37. Parry, D. A., S. V. Strelkov, P. Burkhard, U. Aebi, and H. Herrmann. 2007. Towards a molecular description of intermediate filament structure and assembly. *Exp. Cell Res.* 313:2204–2216.
38. Lee, D. A., T. Noguchi, M. M. Knight, L. O'Donnell, G. Bentley, et al. 1998. Response of chondrocyte subpopulations cultured within unloaded and loaded agarose. *J. Orthop. Res.* 16:726–733.
39. Friedl, G., H. Schmidt, I. Rehak, G. Kostner, K. Schauenstein, et al. 2007. Undifferentiated human mesenchymal stem cells (hMSCs) are highly sensitive to mechanical strain: transcriptionally controlled early osteo-chondrogenic response in vitro. *Osteoarthritis Cartilage.* 15:1293–1300.
40. Wang, N., and D. Stamenovic. 2000. Contribution of intermediate filaments to cell stiffness, stiffening, and growth. *Am. J. Physiol. Cell Physiol.* 279:C188–C194.
41. Brangwynne, C. P., F. C. MacKintosh, S. Kumar, N. A. Geisse, J. Talbot, et al. 2006. Microtubules can bear enhanced compressive loads in living cells because of lateral reinforcement. *J. Cell Biol.* 173:733–741.
42. Putnam, A. J., K. Schultz, and D. J. Mooney. 2001. Control of microtubule assembly by extracellular matrix and externally applied strain. *Am. J. Physiol. Cell Physiol.* 280:C556–C564.
43. Urban, J. P., A. C. Hall, and K. A. Gehl. 1993. Regulation of matrix synthesis rates by the ionic and osmotic environment of articular chondrocytes. *J. Cell. Physiol.* 154:262–270.
44. Pritchard, S., B. J. Votta, S. Kumar, and F. Guilak. 2008. Interleukin-1 inhibits osmotically induced calcium signaling and volume regulation in articular chondrocytes. *Osteoarthritis Cartilage.* 16:1466–1473.
45. Fung, Y. C. 1993. Biomechanics: Mechanical Properties of Living Tissues, 2nd ed. Springer-Verlag, New York.
46. Shieh, A. C., and K. A. Athanasiou. 2007. Dynamic compression of single cells. *Osteoarthritis Cartilage.* 15:328–334.
47. Li, T. 2008. A mechanics model of microtubule buckling in living cells. *J. Biomech.* 41:1722–1729.
48. Kikumoto, M., M. Kurachi, V. Tosa, and H. Tashiro. 2006. Flexural rigidity of individual microtubules measured by a buckling force with optical traps. *Biophys. J.* 90:1687–1696.
49. Tolic-Norrelykke, I. M. 2008. Push-me-pull-you: how microtubules organize the cell interior. *Eur. Biophys. J.* 37:1271–1278.
50. Burbank, K. S., and T. J. Mitchison. 2006. Microtubule dynamic instability. *Curr. Biol.* 16:R516–R517.
51. Coughlin, M. F., and D. Stamenovic. 2003. A prestressed cable network model of the adherent cell cytoskeleton. *Biophys. J.* 84:1328–1336.
52. Aufderheide, A. C., and K. A. Athanasiou. 2006. A direct compression stimulator for articular cartilage and meniscal explants. *Ann. Biomed. Eng.* 34:1463–1474.
53. Brown, P. D., and P. D. Benya. 1988. Alterations in chondrocyte cytoskeletal architecture during phenotypic modulation by retinoic acid and dihydrocytochalasin B-induced reexpression. *J. Cell Biol.* 106:171–179.
54. Titushkin, I., and M. Cho. 2007. Modulation of cellular mechanics during osteogenic differentiation of human mesenchymal stem cells. *Biophys. J.* 93:3693–3702.
55. Lacy, B. E., and C. B. Underhill. 1987. The hyaluronate receptor is associated with actin filaments. *J. Cell Biol.* 105:1395–1404.
56. Knight, M. M., J. M. Ross, A. F. Sherwin, D. A. Lee, D. L. Bader, et al. 2001. Chondrocyte deformation within mechanically and enzymatically extracted chondrons compressed in agarose. *Biochim. Biophys. Acta.* 1526:141–146.
57. Alexopoulos, L. G., L. A. Setton, and F. Guilak. 2005. The biomechanical role of the chondrocyte pericellular matrix in articular cartilage. *Acta Biomater.* 1:317–325.
58. Ofek, G., V. P. Willard, E. J. Koay, J. C. Hu, P. Lin, et al. 2009. Mechanical characterization of differentiated human embryonic stem cells. *J. Biomech. Eng.* 131:061011.